Design of an energy function based fuzzy tuning controller for HVDC links

P.K. Dash[a,*], A. Routray[a], A.C. Liew[b]

[a]*Department of Electrical Engineering, Regional Engineering College, Rourkela 769 008, India*
[b]*Department of Electrical Engineering, National University of Singapore, Singapore*

Abstract

The paper introduces an energy function based fuzzy tuning method for the controller parameters of an HVDC transmission link. The test system, a point to point DC link, was subjected to various small and large disturbances to examine the effectiveness of the proposed method. The DC current error and its derivative are taken as the two principal signals to generate the change in the proportional and the integral gains of the rectifier current regulator according to a fuzzy rule base. Computer simulation results confirm the superiority of the proposed adaptive fuzzy controllers over the conventional fixed gain controllers in damping out the transient oscillations in HVDC links connected to weak AC systems.

Keywords: Fuzzy tuning controller; Computer simulation; Fixed gain controller

1. Introduction

For complex nonlinear and dynamic systems the simplest yet robust controllers are P–I types. Very often in such systems, under certain circumstances, with fixed values of proportional and integral gains, these controllers cause instability. However, with proper tuning of the controller parameters the situations described earlier can be easily overcome. Therefore, the prime objective of the controller design is to adjust the effective proportional, integral and the derivative gains for stable operation of the plant under all possible conditions.

The operation and control of a HVDC link connected to weak AC system is too complex to visualize from a system point of view. The main objective of the DC link controllers at either end (rectifier and inverter) is to operate the link effectively and efficiently.

To get rid of the difficulties during abnormal operating conditions particularly in the presence of weak AC systems extensive research was carried out in the area of HVDC control. Elaborate literature available in DC adaptive control are not very conclusive for all practical situations because of the absence of insight into performance with large disturbances where the adaptive control not only may be ineffective, but may degrade the performance rather than enhance it [1,2].

Reeve et al. have tried a gain scheduling adaptive control where the effect of large disturbances was taken into account [3]. Hammad et al. [4] have proposed a robust coordinated control scheme for a parallel AC–DC system. The paper describes the derivation and validation of a co-ordinated controller based as on-line identification of the AC/DC system parameters. Alexandridis et al. [5] have used Kalman filtering approach for designing the rectifier current regulator in the presence of unknown inputs.

Most of the controllers described earlier, although superior to the conventional PI type, need an accurate plant model as well as a reliable instrumentation scheme. The noise rejection property of these controllers is rather limited.

Recently, extensive research in the area of fuzzy logic control throws some light on its application to large nonlinear systems. In order to account for sensor noise, model uncertainties, and shifts in operating points, the linguistic characteristics of fuzzy controller provide a very good approach to deal with [6–9]. Fuzzy logic control proves to be highly effective in controlling plants whose detailed and accurate mathematical descriptions are not available. Further, fuzzy rules derivation, by principle, relies on the experience of a human expert; which sometimes limits the fuzzy logic controller to lower order systems. Till date such types of controllers have proven

* Corresponding author.

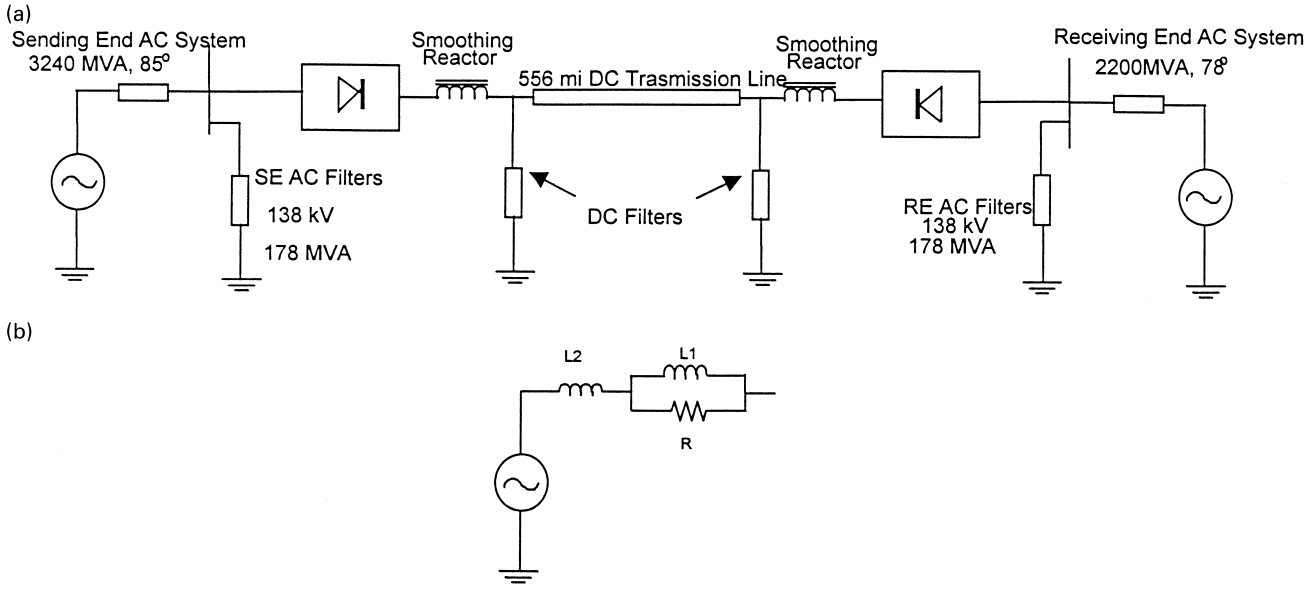

Fig. 1. (a) HVDC system model; (b) Details of AC system representation.

themselves successful in controlling small nonlinear plants. For large systems it still remains a challenge to replace the conventional controllers completely. Therefore to get the advantage of a fuzzy controller without replacing the PI controller, the best way is to dynamically adjust the PI gains by a scheme based on fuzzy logic.

The paper presents an energy function based fuzzy logic approach for on-line tuning of the control parameters for a point-to-point HVDC link connected to a weak AC system. An energy function of the reduced order state-space was chosen. The magnitude and sign of the function and its time derivative determine the change in proportional and integral gains. Finally a comparative study was taken up to demonstrate the feasibility and effectiveness of the proposed scheme with the conventional fixed gain controller.

2. HVDC system model

Particularly in the last 10 years, a wide variety of HVDC converter control strategies were tested and optimized with the help of various digital simulation programs. In 1985 the great interest in HVDC system simulation led to the idea of establishing an HVDC benchmark model [10,11]. In the following years a comparison of one physical simulator and four digital simulation models, were carried out [12,13]. Comparative results from the various simulation programs agreed quite well with the reference simulator results.

For HVDC control and system fault studies a time-step of 50 μs is customarily chosen. This time-step is slightly more than 1° for a 60 Hz waveform and can result in the generation of noncharacteristic harmonics. This difficulty is eliminated if the thyristor switchings are interpolated to within a fraction of time-step. We, therefore, chose to use an EMTP-type program capable of such interpolations such as EMTDC.

The originally proposed 12-pulse point-to-point HVDC benchmark model is slightly modified to provide 6-pulse operation for testing the performance of the fuzzy controllers. The filters, transmission line, and transformers, etc., are represented in detail on either side of the DC link. The system described in Fig. 1 is divided into four subsystems.

2.1. Subsystem I

The rectifier side subsystem consists of inductance and resistance to represent a simplified AC system. The short circuit ratio (SCR) for the system is fairly high as compared to the inverter side AC system. AC filters for 5th, 7th, 11th and 13th harmonics were provided on the rectifier AC bus.

2.2. Subsystem II

The rectifier is connected to the DC transmission line through a large inductor and a 6th harmonic filter was connected to take care of the ripples in the DC voltage.

2.3. Subsystem III

It is identical with the subsystem II except for the fact that it comes in between the inverter and the DC link.

2.4. Subsystem IV

The inverter side AC system representation is identical to that of the rectifier side. The same filters are also present here. But the voltage ratings and SCR are different. The inverter AC side is weaker having an SCR around 3.5.

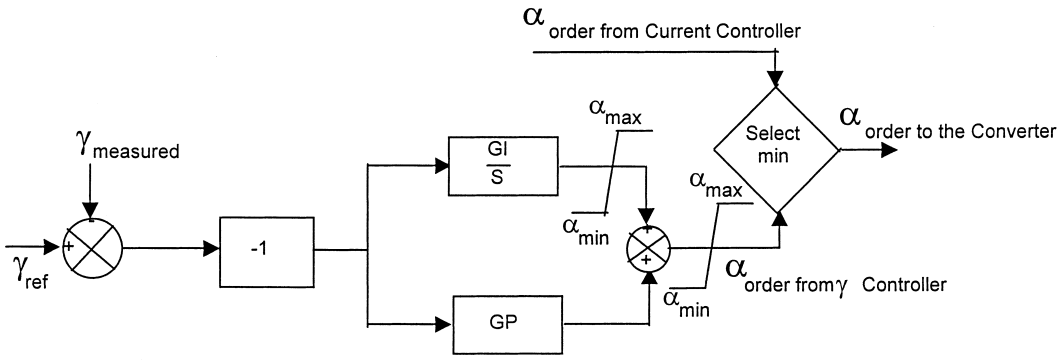

Fig. 2. Inverter gamma controller.

2.5. Converters

The converters on the either side of the DC link were represented by the in-built EMTDC subroutines. It takes care of the simulation of a phase locked loop (PLL) based equidistant pulse control (EPC) scheme for the 6-thryristors.

2.6. Inverter control System (Fig. 2)

The inverter is subjected to extinction angle control as usual. However, a constant current controller was also provided to make the inverter operate in constant current mode under some of the emergency and transient conditions.

2.7. Rectifier control system (Fig. 3)

The DC link current is maintained constant by subjecting the rectifier with constant current control. The firing angles of the valves are adjusted to maintain a DC voltage so as to make the DC line current constant. It is also provided with a constant extinction angle controller for operating under transient and emergency situations.

3. Design implementation

In order to exploit the advantages of the fuzzy controller and also to operate within the stable region, the PI controllers can be tuned by a supervision based on fuzzy logic. By fixing the upper and lower boundary of the PID gains the controller can operate within the stable region. Some of the states of the plant can be processed by the fuzzy supervisor to generate the change in PID gains. To be more precise, a performance index based on an energy function can be monitored by the fuzzy supervisor to generate the change in the PID gains.

3.1. The fuzzy tuner

The energy function rather than the error signal was considered for the adjustment of the gains. When the energy of the error signal (a function of error and rate of change of error) is high then the system is in transient state and therefore, the proportional gain should be adjusted. When the energy is low but not zero, and the system is reaching steady state then the integral gain should be adjusted to bring the system quickly to the equilibrium state. To implement it the following approach based on a quadratic performance index was used. Since the fuzzy rules are derived from a stabilization criterion rather than to satisfy the stabilization criterion, the approach should be inherently stable. Now a method for fuzzy rule design based on the well-known concept of stability in the sense of Lyapunov is presented here. However, while deriving the fuzzy rules it is assumed that, the deviation from the operating point at each iteration, where a new ΔK_p is being issued by the fuzzy rule set, is within the domain of attraction of the (stabilized) closed-loop system. The following energy function is formulated from the current error and its derivative for adjusting the parameters of the Rectifier Current Regulator.

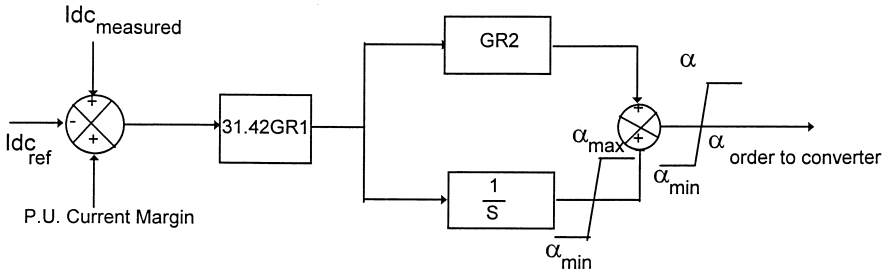

Fig. 3. Rectifier current controller.

Table 1
Proportional gain[a]

$\dot{V}$ \ V	P*	SP	Z
P	N	N	Z
Z	P	Z	Z
N	N	N	Z

[a] P – Positive; SP – Small Positive; Z – Zero; N – Negative; PL – Positive Large; PM – Positive Medium.

Let

$$\Delta I_{dc}(t_k) = I_{dcrf} - I_{dc}(t_k), \tag{1}$$

$$\Delta \dot{I}_{dc}(t_k) = \frac{(\Delta I_{dc}(t_k) - \Delta I_{dc}(t_{k-1}))}{t_k - t_{k-1}} \tag{2}$$

where, I_{dcrf} is the reference current; and $I_{dc}(t_k)$, $I_{dc}(t_{k-1})$ the measured dc link current at instants t_k and t_{k-1} respectively;

$$V = EAE^{T} \tag{3}$$

where

$$E = [\Delta I_{dc} \Delta \dot{I}_{dc}], \qquad A = \begin{bmatrix} a_{11} & 0 \\ 0 & a_{22} \end{bmatrix}$$

is a positive definite matrix for normalizing V.

Here at each instant the energy function depends on the current error which is a measurable quantity, and its derivative, which can be determined through successive measurements of the current error.

The rate of change of V is obtained as

$$\dot{V} = \left(\frac{V(t_k) - V(t_{k-1})}{t_k - t_{k-1}} \right) \tag{5}$$

where, $V(t_k)$, $V(t_{k-1})$ are energy functions at sampling instants t_k and t_{k-1} respectively.

In order to satisfy the stabilization objective, it requires,

$$\dot{V} \le 0 \qquad or \qquad \Delta V \le 0. \tag{6}$$

To derive the fuzzy rule base for the tuning of the proportional and integral gains the following facts are kept in mind:

- When the energy V and the rate of change of energy $\dot{V}$ are both large positive the system is in transient state and diverging away from the equilibrium point. Therefore, the proportional gain is to be increased to damp out the oscillations. On the contrary the integral gain is decreased as it deteriorates the transient performance.
- When the energy V is large positive and the rate of change $\dot{V}$ is small positive the system is in transient state but returning towards the equilibrium point. Therefore, the proportional gain is only given a small increment to accelerate the recovery. Large change in proportional gain may make the system oscillatory. The integral gain remains unchanged.
- When the energy is positive and the rate of change is small negative or positive the system is said to be near the equilibrium point. Therefore, the system has almost reached the steady state. Now the proportional gain is fixed and the integral gain is adjusted to improve the steady state performance.

Table 2
Integral gain[a]

$\dot{V}$ \ V	P*	SP	Z
P	PL	PL	PM
Z	PM	Z	Z
N	Z	Z	Z

[a] P – Positive; SP – Small Positive; Z – Zero; N – Negative.

These facts lead to the fuzzy rule tables (Tables 1 and 2).

After the measurement of error the energy functions are calculated by the fuzzy logic device. These are pre-multiplied by the normalizing gains as shown in Fig. 4 to generate the signals to the fuzzification block. With these fuzzified inputs the inference engine makes use of the appropriate rules to generate the membership grades for the output fuzzy sets. The membership grades for input and outputs are shown in Fig. 5. From the output fuzzy sets and the generated membership grades the actual value of the output (change in proportional and integral gains) are calculated by the center of area defuzzification method as:

$$K_1 = \frac{\Sigma \mu_i y_i}{\Sigma \mu_i} \tag{7}$$

where K_1, K_2 are the output of the fuzzy controller (proportional and integral gain coefficients); μ_i membership grades of the ith output fuzzy set; y_i the numerical value of the output for which the membership grade for the ith fuzzy set is 1.

The values of the GR_1 and GR_2 (Fig. 3) are calculated from the output of the fuzzy tuner as

$$GR_1 = GR_1{}^* + \Delta K_i, \tag{8}$$

$$GR_2 = (GR_1{}^* \cdot GR_2{}^* + \Delta K_p)/GR_1 \tag{9}$$

where $GR_1{}^*$ and $GR_2{}^*$ are the nominal values of the gains, and ΔK_P and ΔK_I are obtained as

$$\Delta K_p = GU_p \cdot K_1, \qquad \Delta K_1 = GU_1 \cdot K_2. \tag{10}$$

Limits of 50%–200% are put on the gains to keep the system in a stable region. The limits were found out by trial and error.

Further to satisfy the energy function gradient conditions given by Eq. (6), the following conditions are checked at every sampling instant t_k:

$$\text{sign}(\Delta\alpha(t_{k+1}) = -\text{sign}\left(\frac{\partial V}{\partial \alpha}(t_k) \right) \tag{11}$$

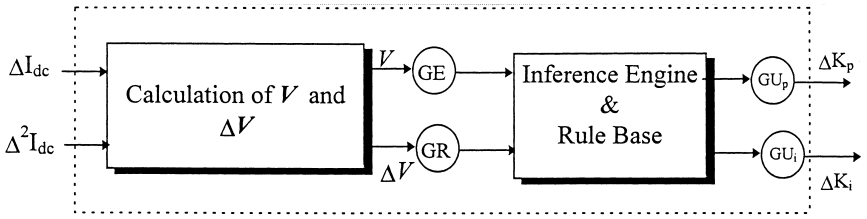

Fig. 4. Energy function based fuzzy logic device for the adaption of K_p and K_i.

which leads to

$$\Delta V(t_{k+1}) \approx \left(\frac{\partial V}{\partial \alpha}(t_k)\right)\Delta\alpha(t_{k+1}) < 0. \tag{12}$$

The value of $(\partial V/\partial\alpha)(t_k)$ is calculated as

$$\frac{\partial V}{\partial \alpha}(t_k) \approx \frac{\Delta V(t_k)}{\Delta\alpha(t_k)} = \frac{V(t_k) - V(t_{k-1})}{\alpha(t_k) - \alpha(t_{k-1})}. \tag{13}$$

After designing the fuzzy tuner it is tested for various faults and other disturbances on the system. The waveforms resulting from these studies are shown in Figs. 6–10. The comparative results are discussed in the following paragraphs.

The parameters of the tuner described earlier are the normalizing gains at the input and output, the number of input and output fuzzy sets, the nature of the membership functions and the inference method, etc. For the best performance of the tuner, it is mandatory to choose an optimum set of values. However, the structure of the controller, which is determined by the rule base and the number of fuzzy sets are chosen byof trial and error. The nature of the membership functions is assumed to be linear. Now the rest of the parameters (mainly the normalizing gains) are determined by minimizing a performance index (PI) given by

$$\mathrm{PI} = \int_0 z^2(\Delta I_{\mathrm{dc}}(z))^2\, \mathrm{d}z \tag{14}$$

which is the integral time square error (ITSE) of the current error. The simulation program is run repeatedly under different types of disturbances for different values of gains. The ITSE for each run is calculated and the value of the gain for the minimum value of the ITSE is chosen.

4. Results and discussion

To test the effectiveness of the controllers discussed above the system was subjected to the following types of disturbances:

1. Single line-to-ground fault at the inverter AC bus;
2. Three phase-to-ground fault at the rectifier bus;
3. DC line-to-line fault at the inverter end;
4. Step change in the rectifier current order; and
5. Single line-to-ground fault at the inverter AC bus with change in the short circuit ratio.

4.1. Single-line-to-ground fault at the inverter AC bus

A single-line-to ground fault was created in the Inverter AC system for about five cycles. The inverter end AC system is weaker than the rectifier end AC system with a short circuit ratio around 3.5. Therefore, such kinds of faults lead to sudden voltage collapse on all the other phases

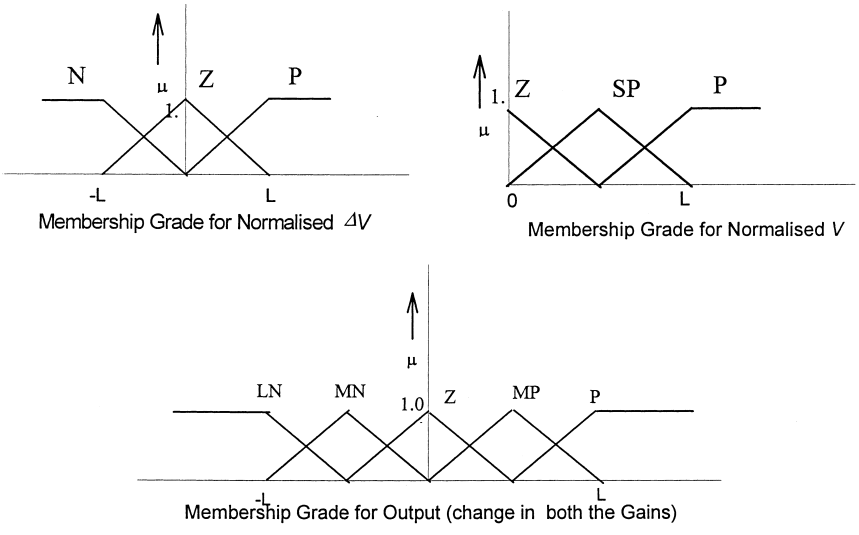

Fig. 5. Membership grades for input and output in fuzzy tuner.

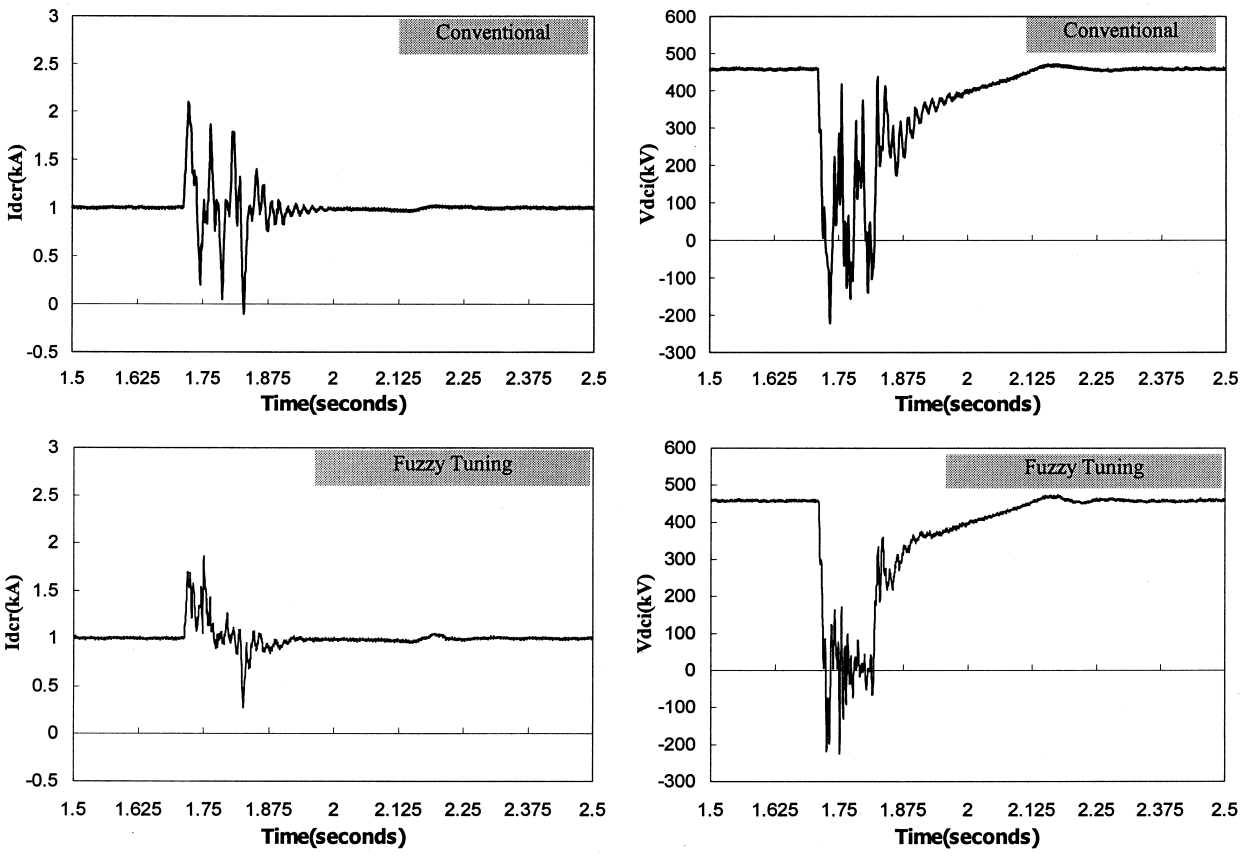

Fig. 6. Single-line-to-ground fault at inverter AC bus.

leading to commutation failures and other difficulties in the converter operation. This also leads to unbalanced operation of the converter even after the fault is cleared. The Inverter DC voltage plots (Fig. 6) indicate a number of commutation failures of the corresponding valve groups. The firing instants are now uncertain and hence the Inverter Gamma controller loses control over the DC link recovery. The transient performance under this condition is mostly influenced by the rectifier current regulator. Therefore the comparative study shows substantial difference in the plant response for different types of controllers. From the simulation waveforms it can be concluded that

- The fuzzy tuner exhibits far better performance in comparison to the conventional current regulator. In this case the oscillations in the DC link current, voltage and above all the oscillations in DC link power were minimized to a greater extent.

4.2. Three-phase-to-ground fault at the rectifier bus

Waveforms resulting from a three-phase-to-ground fault at the rectifier is displayed in Fig. 7. Here the rectifier bus voltage completely collapses and results in commutation failure of converter valves. During the fault the DC current drops to zero and the firing angle settles at the minimum value. The zero current and zero power condition lead to complete collapse of the DC link. As soon as the fault is cleared the current controller gets activated. And it is in this period that the link operation is influenced by the controller actions.

From the comparative study presented in the following paragraphs it can be further concluded that:

- The current controller is almost defunct as the firing angle hits the minimum limit. It is activated only when the fault is cleared. Therefore only a little improvement is observed in the waveforms resulting from the proposed controller actions.

4.3. DC line-to-line fault at the inverter

Fig. 8 shows the waveforms after a five-cycle DC line-to-line fault at the inverter. This kind of fault is most severe when the connected AC system is weak. The nature of the fault is balanced but most critical owing to the low SCR of the inverter AC system. This is in a way similar to a three-phase fault at the inverter bus, since the total power injection becomes zero. The oscillations may give rise to uncontrolled dv/dt and di/dt stress on the converter valves. Also the oscillations on the inverter bus voltage (AC) may be detrimental to the industrial or other loads connected. As

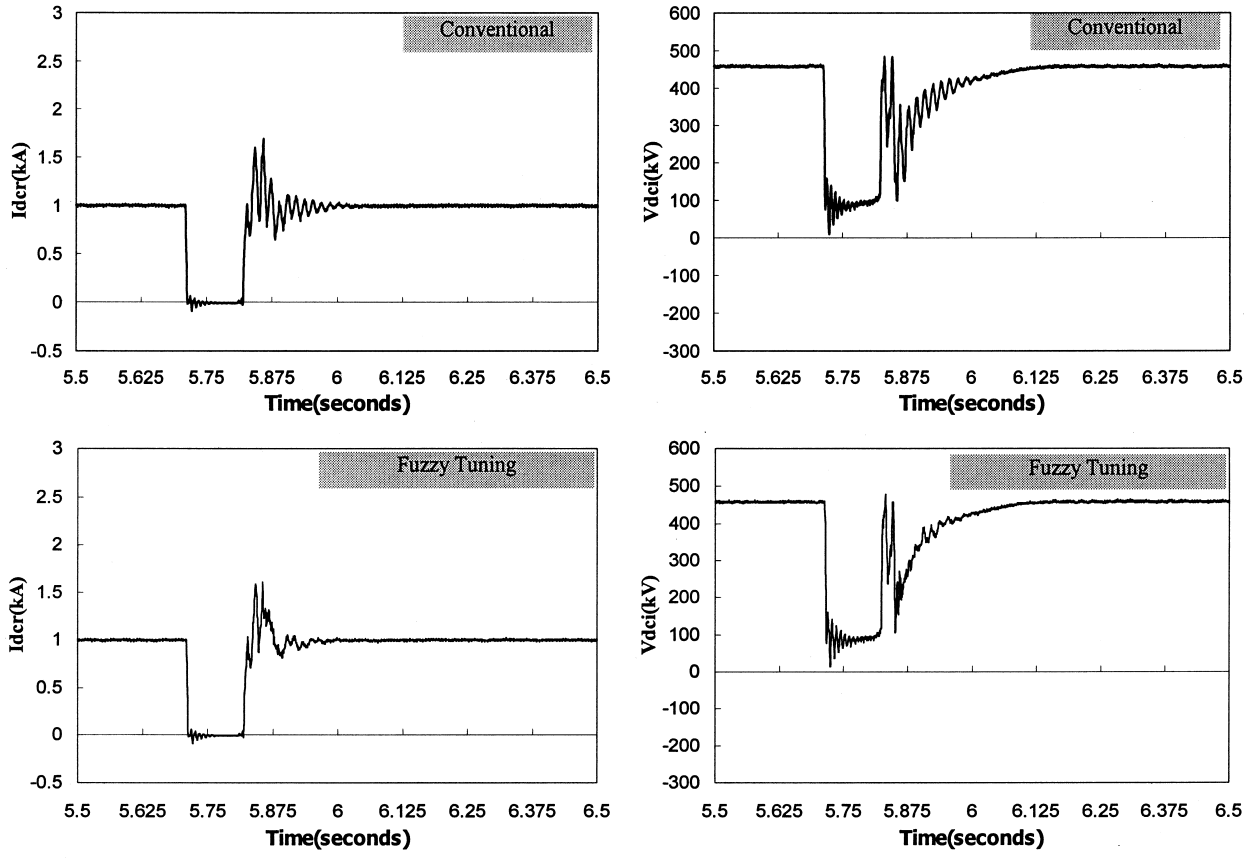

Fig. 7. Three-phase-to-ground fault at rectifier AC bus.

seen from Fig. 9 the conventional controller makes the system oscillate after the fault is removed. In this case, since the current error becomes higher the rectifier-firing angle hits the maximum limit. Consequently the current regulator virtually becomes temporarily ineffective. From the comparative results it is concluded that:

- The DC link behavior is primarily decided by the action of the gamma controller rather than the rectifier current regulator.
- However, the oscillations were minimized in case of fuzzy tuner.

4.4. Single-line-to-ground fault at inverter AC bus with simultaneous change in SCR

The parameters of the controllers described earlier were optimized for the nominal value of the inverter and rectifier end short circuit impedance of the AC systems. To test the sensitivity of the proposed controllers to the parameter variation, the short circuit impedance of the inverter end AC system is changed to a different value after a five-cylce single line to ground fault on the inverter AC bus.

The nominal value (the controller gains are optimized at this value) (Fig. 1):

$L_1 = 0.00767$ H, $L_2 = 0.002735$ H, $R = 1.267\ \Omega$

(Rectifier AC system SCR $= 22\angle 81.8°$),

$L_1 = 0.0443$ H, $L_2 = 0.0277$ H, $R = 14.2\ \Omega$

(Inverter AC system SCR $= 3.25\angle 78°$).

The changed value after the fault is cleared:

$L_1 = 0.00767$ H, $L_2 = 0.02735$ H, $R = 1.267\ \Omega$

(Rectifier AC system SCR $= 22\angle 81.8°$),

$L_1 = 0.0443$ H, $L_2 = 0.08$ H, $R = 50\ \Omega$

(Inverter AC system SCR $= 1.9\angle 71°$).

Several commutation failures can be easily assessed from the oscillations in the Inverter DC voltage plots (Fig. 9). The comparative study from the voltage and current waveforms clearly shows the advantages of the proposed controller.

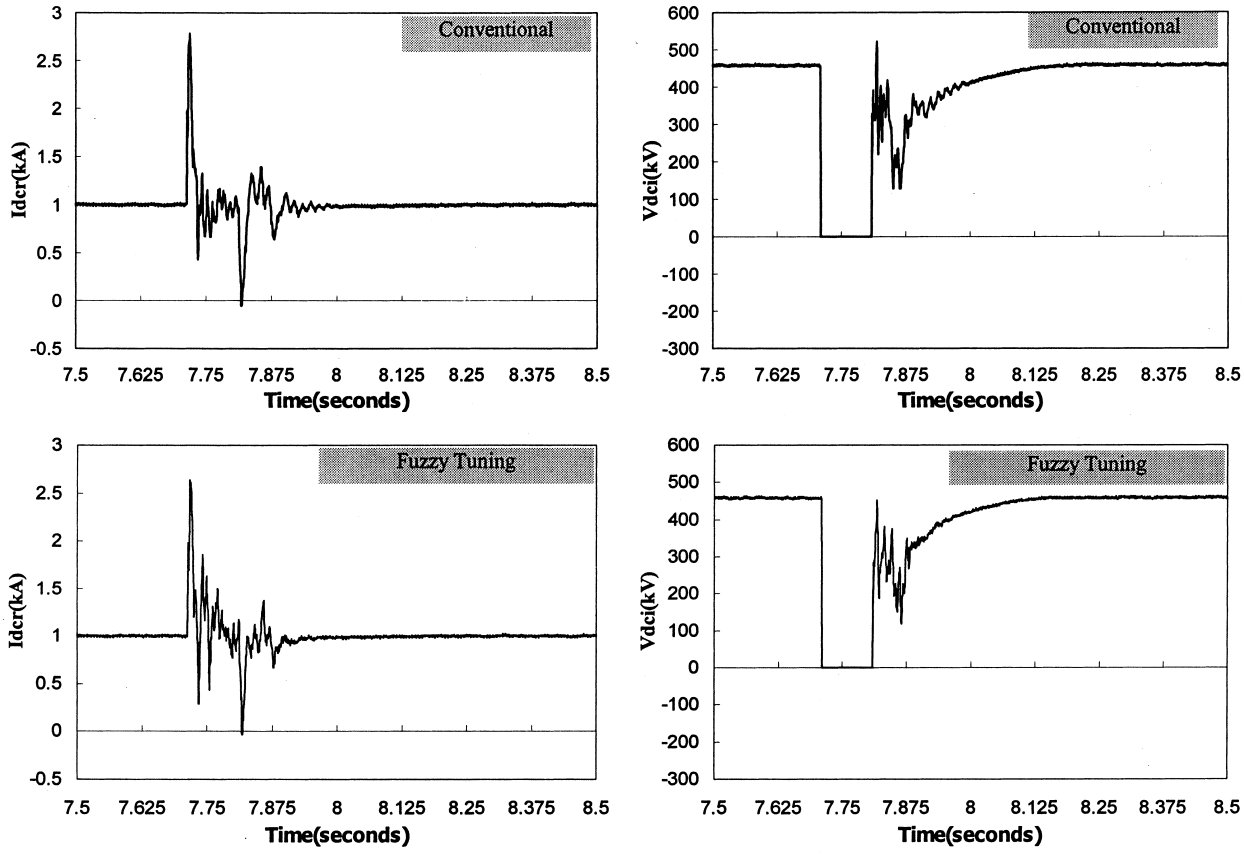

Fig. 8. DC-line-to-line fault at inverter.

4.5. Step change in rectifier current order

The rectifier current regulator is subjected to a step change. The reference is decreased from 1 to 0.5 p.u. and then increased to 1.0 p.u. The response of the system under various controller actions is shown in Fig. 10. This is treated as a normal disturbance, which occurs very often whenever the DC link power is increased or decreased. Therefore it is always desirable to keep the system in operation with little transient in DC link power and voltage waveforms. The conventional controller shows a lot of transients with the step change. The DC link power falls momentarily to zero, whereas with the proposed controller there is only a little disturbance before the current and power settles down at the new value.

5. Conclusion

In this paper the performance of a point-to-point HVDC link is studied using a fuzzy tuner. An energy function based fuzzy tuner was proposed for the rectifier current regulator. Owing to the nonavailability of any standard design technique the control parameters are determined first by trial and error and then further tuned by optimization of integral square error.

From the above simulation results it is further concluded that

1. The rectifier side AC-system being strong, recovers very fast after any type of disturbance, overriding the effect of most of the controller actions. Therefore, for any type of fault on the rectifier AC or DC bus, much difference is not observed in the current and voltage waveforms for most of the controller actions.
2. For the faults in the inverter side, the proposed controller makes the system recover much faster than the conventional PI controller does. The commutation failures, power oscillations and high d*i*/d*t*, which are detrimental to the converter operation were minimized in case of the proposed controller.
3. It is also observed that the operation of the DC link is very sensitive to the change in short-circuit ratio. Under such conditions the DC link operation was much improved with the proposed controller.

For HVDC links where very large transient conditions are involved in the plant operation, it is more convenient to improve the PI control strategy rather than to work out complicated dynamic models, which require sophisticated control strategies. The application of the linguistic rules is in fact simpler than sophisticated identification and optimization procedures. The implementation of fuzzy controllers is

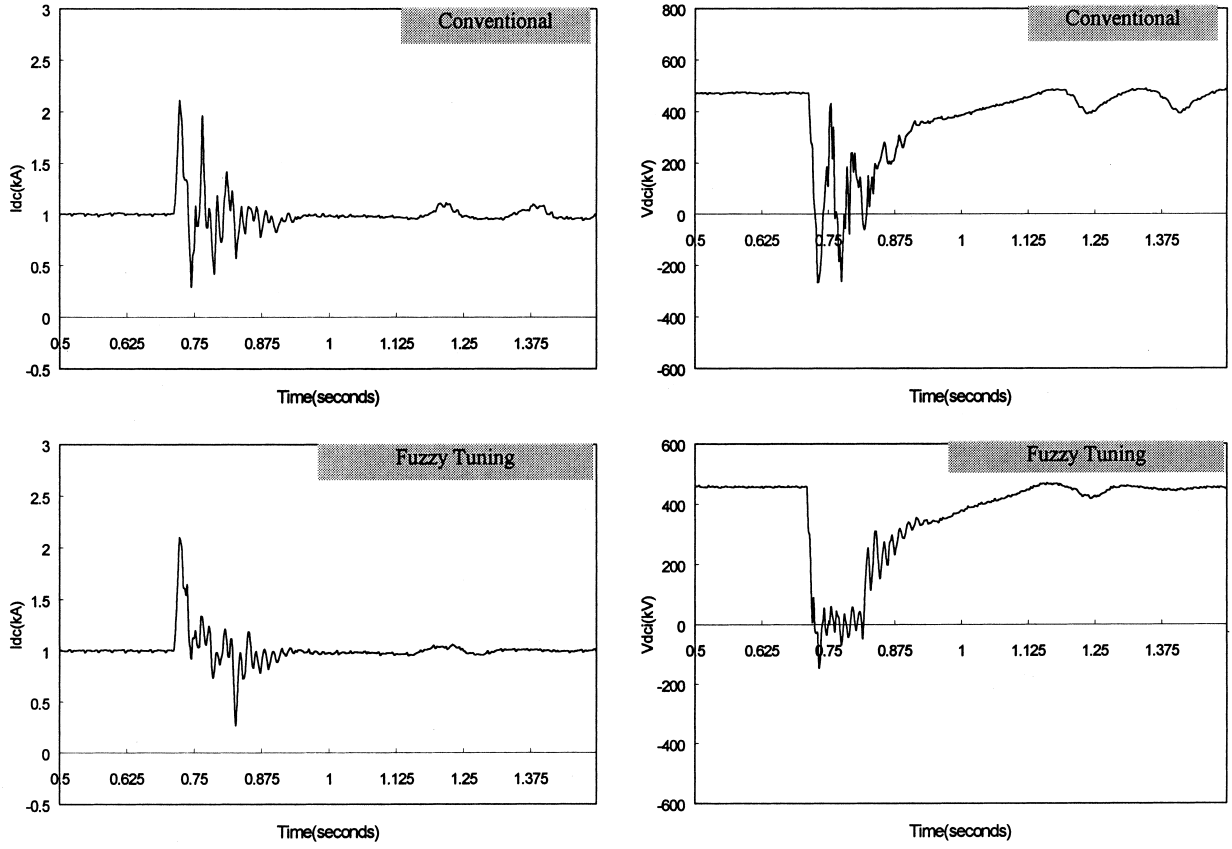

Fig. 9. Single-line-to-ground fault at inverter AC bus (with simultaneous change of SCR).

also less complicated than that of optimization algorithms. The results obtained are quite encouraging and the application in real life will depend on the development of an acceptable theoretical base for designing the complete structure of these controllers.

Acknowledgements

Funds for this project from the Department of Science and Technology, Government of India is acknowledged.

Appendix A

Data for the system model are provided below.

A.1. Rectifier end AC system

Data for the AC filters at the rectifier end (200 kV) are shown in Table 3. The rectifier end AC system consists of a constant voltage and constant frequency source behind an L-LR (Fig. 1(b)) network which represents the equivalent Thevenin impedance of the AC network. The short-circuit ratio is approximately 14 representing a strong system. The impedance network consists of: $R = 1.267\,\Omega$, $L_1 = 0.002735$ H, $L_2 = 0.00767$ H.

B.1. Inverter end AC system

The data for the AC filters at the inverter end (340 kV) are shown in Table 4. The inverter end AC system consists of a constant voltage, constant frequency source behind an L-LR Fig. 1(b) network. The short-circuit ratio is roughly 3.5 representing a relatively weak system. The impedance network consists of: $R = 14.2\,\Omega$, $L_1 = 0.0277$ H, $L_2 = 0.0443$ H.

C.1. DC subsystems

Both the inverter and rectifier side subsystems are identical. Each consists of a large inductor in series between the converter and DC transmission line. A DC filter was connected in parallel to take care of DC voltage harmonics. Smoothing inductor: $L_d = 0.75$ H, Filter data: $R = 24.0\,\Omega$, $L = 0.2444$ H, $C = 0.8\,\mu$F (for 6th Harmonic).

D.1. DC transmission line

A 556 mile long transmission line connects the rectifier and inverter DC subsystems. The following data pertains to the details of the line: Steady state lower frequency = 5 Hz; High frequency transient = 90 Hz; Mode traveling time = 3.037 ms; Characteristic impedance = 300 Ω; Mode resistance per unit length at the lower frequency = 0.025 Ω; and

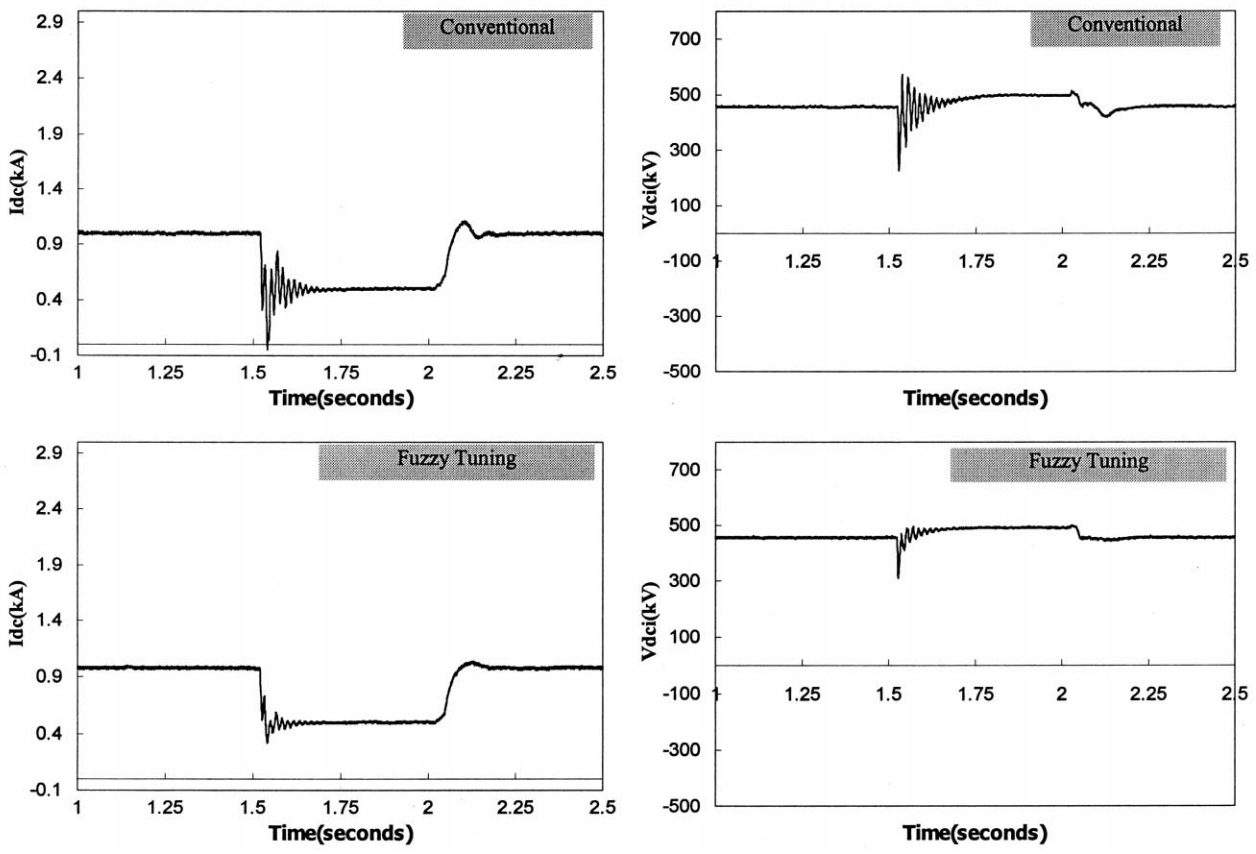

Fig. 10. Step change in rectifier current order.

Table 3
Data for AC filters at rectifier (178 MV A)

n	5th	7th	11th
R (Ω)	2.0	3.0	2.0
L (H)	0.0614	0.0614	0.0152
C (μF)	4.58	2.337	3.84

Table 4
Data for AC filters at inveter (178MV A)

n	5th	7th	11th
R (Ω)	8.0	8.0	3.0
L (H)	0.168	0.168	0.0444
C (μF)	1.67	0.852	1.310

Mode resistance per unit length at the higher frequency = 0.03 Ω.

E.1. Pole controller

For the conventional pole controller on the either side: $GR_1 = 5.88$, $GR_2 = 0.0136$. Rectifier pole controller: $\alpha_{min} = 5°$, $\alpha_{max} = 155°$ Inverter pole controller: $\alpha_{min} = 108°$, $\alpha_{max} = 178°$.

F.1. Valve controller

For the conventional PI type gamma controller on the either side: GP = 0.27, GI = 15.0.

References

[1] Lefebvre S, Saad M, Hurteau AR. Adaptive control for HVDC power transmission systems. IEEE Transactions on Power Apparatus and Systems 1985;PAS-104(9):2329–2335.
[2] Rugh WJ. Analytical framework for gain scheduling. IEEE Control Systems Magazine 1991;II(1):79–84.
[3] Reeve J, Sultan M. Gain scheduling adaptive control strategies for HVDC systems to accommodate large disturbances. IEEE Transactions on Power Systems 1994;9(1):366–372.
[4] To KWV, David AK, Hammad AE. A robust co-ordinated control scheme for HVDC transmission with parallel AC systems. IEEE 94WM 061-2 PWRD.
[5] Alexandridis AT, Galanos GD. Design of an optimal current regulator for weak AC/DC systems using Kalman filtering in the presence of unknown inputs. IEE Proceedings 1989;136(2):57–63.
[6] De carli A, Ligouri P, Marroni A. A fuzzy-PI control strategy. Control Engineering Practice 1994;2(1):147–153.
[7] Sood VK, Kandil N, Patel RV, Khorasani K. Comparative evaluation of neural network based and PI current controllers for HVDC transmission. IEEE Transactions on Power Electronics 1994;9(3):288–295.
[8] Chris Tseng H, Victor Hwang, Sung Lep Lui. Fuzzy servocotroller: the hierarchical approch. 0-7803-0236-2/92 ©IEEE, pp. 623–631.

[9] Chris Tseng H, Hwang V. Servocontroller tuning with fuzzy logic. IEEE Transactions on Control System Technology 1994;1(4):262–269.
[10] EMTDC User's Manual. Winnipeg, MB, Canada: Manitoba HVDC Research Center.
[11] Ainsworth JD. Proposed benchmark model for study of HVDC simulator or digital computer presented at the CIGRE SC-14 colloquium on HVDC with weak AC systems, UK, September 1985.
[12] Szechtman M et.al. First benchmark model for HVDC control studies. Electra 1991;135:54–67.
[13] Rittiger J. Digital simulation of HVDC transmission and correlation to simulator studies. IEE Conference Publication Number 34, pp. 414–416.